Journal of Achievements in Materials and Manufacturing Engineering
VOLUME 16
ISSUE 1-2
May-June
2006

Optimisation of autofrettage in thick-walled cylinders

G.H. Majzoobi*, A. Ghomi
Mechanical Engineering Department, Faculty of Engineering,
Bu-Ali Sina University, Hamadan, Iran
* Corresponding author: E-mail address: gh_majzoobi@yahoo.co.uk

Received 15.11.2005; accepted in revised form 15.04.2006

Analysis and modelling

ABSTRACT

Purpose: The purpose of this paper is optimization of the weight of compound cylinder for a specific pressure. The variables are shrinkage radius and shrinkage tolerance.

Design/methodology/approach: SEQ technique for optimization, the finite element code, ANSYS for numerical simulation are employed to predict the optimized conditions. The results are verified by testing a number of closed end cylinders with various geometries, materials and internal pressures.

Findings: The weight of a compound cylinder could reduce by 60% with respect to a single steel cylinder. The reduction is more significant at higher working pressures. While the reduction of weight is negligible for $k<2.5$, it increases markedly for $2.5<k<5.5$. The stress at the internal radii of the outer and inner cylinders become equal to the yield stresses of the materials used for compound cylinders. The experimental results showed higher bursting pressure for optimized cylinders.

Research limitations/implications: The research must be done for non-linear material models and for multiple compound cylinders.

Practical implications: The results can be used for high pressure vessels such as artillery tubes, gun barrels and son on.

Originality/value: The numerical results indicated that for an optimum condition, the stress at the internal radii of the outer and inner cylinders become equal to the yield stresses of the materials used for compound cylinders.

Keywords: Analysis and modelling; Numerical techniques; Compound cylinder; Optimisation; Finite element method

1. Introduction

Autofrettage is an elastic-plastic techniques to increase the pressure capacity of thick-walled cylinders. In this technique, the cylinder is subjected to an internal pressure so that its wall becomes partially plastic. The pressure is then released and the resulting residual stresses increase the pressure capacity of the cylinder in the next loading stage [1 & 2]. The analysis of residual stresses and deformation in an autofrettaged thick-walled cylinder has been given by Chen [3] and Franklin and Morrison [4].

In autofrettage, the key problem is to determine the appropriate the optimum of the radius of elasto-plastic junction to be called r_{opt} in this paper and the autofrettage pressure, p_{opt}.

In the results reported by Harvey [6], no detailed result but only a concept about autofrettage was given. Brownell and Young [7], and Yu [8] proposed a repeated trial calculation method to determine r_{opt} which were a bit too tedious and inaccurate; moreover this method is based on limiting only hoop stress and is essentially based on the first strength theory which is in agreement with brittle materials, while pressure vessels are made generally from ductile materials [9 & 10] which are in excellent agreement with the third or the fourth strength theory [11 & 13]. The graphic method presented by Kong [12] was also a bit too tedious and inaccurate. The purpose of the present paper is to find out a simple, applicable, and reasonable appraoch to determine r_{opt} which does not appear to be available in the existing literature, and to study problems about autofrettage.

Based on the third and the fourth strength theory, Zhu and Yang [14] presented an analytic equation for optimum radius of elastic-plastic juncture, r_{opt} in autofrettage technology. Their work presented the influence of autofrettage on stress distribution and load-bearing capacity of a cylinder and optimum pressure in autofrettage technology was studied. The work by Zhu and Yang considers only elastic-prefectly material model which obviously is not the case for most of the applications.

According to work given by Zhu and Yang [14], the optimum elaso-plastic radius, r_{opt}, and optimum autofrettage presure, p_{opt}, are calculated from the relations given below:

(a) In view of the third strength theory:

$$r_{opt} = r_i \exp\left(\frac{p}{\sigma_y}\right) \tag{1}$$

$$p_{opt} = \frac{\sigma_y}{2}\left[1-\left(1-\frac{2p}{\sigma_y}\right)\exp\left(\frac{2p}{\sigma_y}\right)\right]+p \tag{2}$$

(b) In view of the fourth strength theory:

$$r_{opt} = r_i \exp\left(\frac{\sqrt{3}p}{2\sigma_y}\right) \tag{3}$$

$$p_{opt} = \frac{\sigma_y}{\sqrt{3}}\left[1-\left(1-\frac{\sqrt{3}p}{\sigma_y}\right)\exp\left(\frac{\sqrt{3}p}{\sigma_y}\right)\right]+p \tag{4}$$

In the present work, the optimization techniques, numerical simulation and experiments are employed to predict the optimized autofretage radius. SEQ technique is used for optimization purposes. A finite element code, is employed for numerical simulations and finally, the results are verified by testing a number of closed end cylinders at various autofrettage pressures. The results are then compared with those given by Zhu and Yang [14]

2. Analytical relations

The distribution of radial and hoop stresses within the elastic region and plastic core can be described as follow:

For elastic perfectly plastic material:

In elastic region, $a \le r \le c$:

$$\sigma_r = \frac{k^2 p_o - p_i}{1-k^2} - \frac{p_o - p_i}{1-k^2}\left(\frac{b}{r}\right)^2 \tag{5}$$

$$\sigma_\theta = \frac{k^2 p_o - p_i}{1-k^2} + \frac{p_o - p_i}{1-k^2}\left(\frac{b}{r}\right)^2 \tag{6}$$

In plastic region, $c \le r \le b$,

$$\sigma_r = \frac{\sigma_y}{2}\left[\left(\frac{c^2}{b^2}-1\right)-\ln\left(\frac{c^2}{r^2}\right)\right] \tag{7}$$

$$\sigma_\theta = \frac{\sigma_y}{2}\left[\left(\frac{c^2}{b^2}+1\right)-\ln\left(\frac{c^2}{r^2}\right)\right] \tag{8}$$

For elastic-plastic material with linear strain hardening:

In plastic region, $a \le r \le c$, for an internal pressure P_i :

$$\sigma_r = -\frac{\sigma_y}{2}\left[\left(1-\frac{c^2}{b^2}\right)+\ln\frac{c^2}{r^2}+(1-\nu^2)\frac{E^p}{E}\left(\frac{c^2}{r^2}-\frac{c^2}{b^2}\right)\right]\Big/\left[1+(1-\nu^2)\frac{E^p}{E}\right] \tag{9}$$

$$\sigma_\theta = \frac{\sigma_y}{2}\left[\left(1+\frac{c^2}{b^2}\right)-\ln\frac{c^2}{r^2}+(1-\nu^2)\frac{E^p}{E}\left(\frac{c^2}{r^2}+\frac{c^2}{b^2}\right)\right]\Big/\left[1+(1-\nu^2)\frac{E^p}{E}\right] \tag{10}$$

When the cylinder is pressurized to the autofrettage pressure and the pressure is removed, the residual stress distribution across the wall of the cylinder can be expressed as follow [15]:

For elastic-perfectly plastic material:

Residual stresses in plastic region $a \le r \le c$:

$$\sigma_{rr} = \frac{\sigma_y}{2}[\frac{c^2}{b^2}-1-\ln\frac{c^2}{r^2}+\frac{b^2}{r^2}\cdot\frac{1}{k^2-1}\left(\ln\frac{c^2}{a^2}+1-\frac{c^2}{b^2}\right) - \frac{1}{k^2-1}\left(\ln\frac{c^2}{a^2}+1-\frac{c^2}{b^2}\right)] \tag{11}$$

$$\sigma_{\theta r} = \frac{\sigma_y}{2}[\frac{c^2}{b^2}+1-\ln\frac{c^2}{r^2}-\frac{b^2}{r^2}\cdot\frac{1}{k^2-1}\left(\ln\frac{c^2}{a^2}+1-\frac{c^2}{b^2}\right) - \frac{1}{k^2-1}\left(\ln\frac{c^2}{a^2}+1-\frac{c^2}{b^2}\right)] \tag{12}$$

Residual stresses in elastic region $c \le r \le b$:

$$\sigma_{rr} = -\frac{\sigma_y}{2}[\frac{c^2}{r^2}-\frac{c^2}{b^2}-\frac{b^2}{r^2}\cdot\frac{1}{k^2-1}\left(\ln\frac{c^2}{a^2}+1-\frac{c^2}{b^2}\right) + \frac{1}{k^2-1}\left(\ln\frac{c^2}{a^2}+1-\frac{c^2}{b^2}\right)] \tag{13}$$

$$\sigma_{\theta r} = \frac{\sigma_y}{2}[\frac{c^2}{r^2}+\frac{c^2}{b^2}-\frac{b^2}{r^2}\cdot\frac{1}{k^2-1}\left(\ln\frac{c^2}{a^2}+1-\frac{c^2}{b^2}\right) - \frac{1}{k^2-1}\left(\ln\frac{c^2}{a^2}+1-\frac{c^2}{b^2}\right)] \tag{14}$$

For elasto-plastic material:

Residual stresses in plastic region $a \le r \le c$:

$$\sigma_{rr} = \frac{\sigma_y\left(\frac{b^2}{r^2}-1\right)\left[1-\frac{c^2}{b^2}+2\ln\frac{c}{a}+(1-\nu^2)\frac{E^p}{E}\left(\frac{c^2}{a^2}-\frac{c^2}{b^2}\right)\right]}{2\left(k^2-1\right)\left[1+(1-\nu^2)\frac{E^p}{E}\right]} - \frac{\sigma_y\left[1-\frac{c^2}{b^2}+2\ln\frac{c}{r}+(1-\nu^2)\frac{E^p}{E}\left(\frac{c^2}{r^2}-\frac{c^2}{b^2}\right)\right]}{2\left[1+(1-\nu^2)\frac{E^p}{E}\right]} \tag{15}$$

$$\sigma_{\theta r}=\frac{-\sigma_y\left(\frac{b^2}{r^2}+1\right)\left[1-\frac{c^2}{b^2}+2\ln\frac{c}{a}+(1-\nu^2)\frac{E^p}{E}\left(\frac{c^2}{a^2}-\frac{c^2}{b^2}\right)\right]}{2\left(k^2-1\right)\left[1+(1-\nu^2)\frac{E^p}{E}\right]}+\frac{\sigma_y\left[1+\frac{c^2}{b^2}-2\ln\frac{c}{r}+(1-\nu^2)\frac{E^p}{E}\left(\frac{c^2}{r^2}+\frac{c^2}{b^2}\right)\right]}{2\left[1+(1-\nu^2)\frac{E^p}{E}\right]} \tag{16}$$

Residual stresses in elastic region $c \le r \le b$:

$$\sigma_{rr}=\frac{\sigma_y\left(\frac{b^2}{r^2}-1\right)\left[1-\frac{c^2}{b^2}+2\ln\frac{c}{a}+(1-\nu^2)\frac{E^p}{E}\left(\frac{c^2}{a^2}-\frac{c^2}{b^2}\right)\right]}{2\left(k^2-1\right)\left[1+(1-\nu^2)\frac{E^p}{E}\right]}-\frac{\sigma_y c^2\left(b^2-r^2\right)}{2b^2r^2} \tag{17}$$

$$\sigma_{\theta r}=\frac{-\sigma_y\left(\frac{b^2}{r^2}+1\right)\left[1-\frac{c^2}{b^2}+2\ln\frac{c}{a}+(1-\nu^2)\frac{E^p}{E}\left(\frac{c^2}{a^2}-\frac{c^2}{b^2}\right)\right]}{2\left(k^2-1\right)\left[1+(1-\nu^2)\frac{E^p}{E}\right]}+\frac{\sigma_y c^2\left(b^2+r^2\right)}{2b^2r^2} \tag{18}$$

If the cylinder is loaded again by the internal working pressure, by superposing the residual stresses due to autofrettage and the working pressure, the final stress distribution in the wall of the cylinder will becomes:

For elastic-prefectly plastic material:
Overall stresses in plastic region $a \le r \le c$:

$$\sigma_{rf}=\sigma_{rr}+\sigma_r=\frac{\sigma_y}{2}\Big[\frac{c^2}{b^2}-1-\ln\frac{c^2}{r^2}+\frac{b^2}{r^2}\cdot\frac{1}{k^2-1}\left(\ln\frac{c^2}{a^2}+1-\frac{c^2}{b^2}\right)-\frac{1}{k^2-1}\left(\ln\frac{c^2}{a^2}+1-\frac{c^2}{b^2}\right)\Big]-p\frac{b^2/r^2-1}{k^2-1} \tag{19}$$

$$\sigma_{\theta f}=\sigma_{\theta r}+\sigma_\theta=\frac{\sigma_y}{2}\Big[\frac{c^2}{b^2}+1-\ln\frac{c^2}{r^2}-\frac{b^2}{r^2}\cdot\frac{1}{k^2-1}\left(\ln\frac{c^2}{a^2}+1-\frac{c^2}{b^2}\right)-\frac{1}{k^2-1}\left(\ln\frac{c^2}{a^2}+1-\frac{c^2}{b^2}\right)\Big]+p\frac{b^2/r^2+1}{k^2-1} \tag{20}$$

Overall stresses in elastic region $c \le r \le b$:

$$\sigma_{rf}=\sigma_{rr}+\sigma_r=-\frac{\sigma_y}{2}\Big[\frac{c^2}{r^2}-\frac{c^2}{b^2}-\frac{b^2}{r^2}\cdot\frac{1}{k^2-1}\left(\ln\frac{c^2}{a^2}+1-\frac{c^2}{b^2}\right)+\frac{1}{k^2-1}\left(\ln\frac{c^2}{a^2}+1-\frac{c^2}{b^2}\right)\Big]-p\frac{b^2/r^2-1}{k^2-1} \tag{21}$$

$$\sigma_{\theta f}=\sigma_{\theta r}+\sigma_\theta=\frac{\sigma_y}{2}\Big[\frac{c^2}{r^2}+\frac{c^2}{b^2}-\frac{b^2}{r^2}\cdot\frac{1}{k^2-1}\left(\ln\frac{c^2}{a^2}+1-\frac{c^2}{b^2}\right)-\frac{1}{k^2-1}\left(\ln\frac{c^2}{a^2}+1-\frac{c^2}{b^2}\right)\Big]+p\frac{b^2/r^2+1}{k^2-1} \tag{22}$$

For elastic-plastic material:
Overall stresses in plastic region $a \le r \le c$:

$$\sigma_{rf}=\frac{\sigma_y\left(\frac{b^2}{r^2}-1\right)\left[1-\frac{c^2}{b^2}+2\ln\frac{c}{a}+(1-\nu^2)\frac{E^p}{E}\left(\frac{c^2}{a^2}-\frac{c^2}{b^2}\right)\right]}{2\left(k^2-1\right)\left[1+(1-\nu^2)\frac{E^p}{E}\right]}-\frac{\sigma_y\left[1-\frac{c^2}{b^2}+2\ln\frac{c}{r}+(1-\nu^2)\frac{E^p}{E}\left(\frac{c^2}{r^2}-\frac{c^2}{b^2}\right)\right]}{2\left[1+(1-\nu^2)\frac{E^p}{E}\right]}-\frac{P\left(\frac{b^2}{r^2}-1\right)}{k^2-1} \tag{23}$$

$$\sigma_{\theta f}=\frac{-\sigma_y\left(\frac{b^2}{r^2}+1\right)\left[1-\frac{c^2}{b^2}+2\ln\frac{c}{a}+(1-\nu^2)\frac{E^p}{E}\left(\frac{c^2}{a^2}-\frac{c^2}{b^2}\right)\right]}{2\left(k^2-1\right)\left[1+(1-\nu^2)\frac{E^p}{E}\right]}+\frac{\sigma_y\left[1+\frac{c^2}{b^2}-2\ln\frac{c}{r}+(1-\nu^2)\frac{E^p}{E}\left(\frac{c^2}{r^2}+\frac{c^2}{b^2}\right)\right]}{2\left[1+(1-\nu^2)\frac{E^p}{E}\right]}+\frac{P\left(\frac{b^2}{r^2}+1\right)}{k^2-1} \tag{24}$$

Overall stresses in elastic region $c \le r \le b$:

$$\sigma_{rf}=\frac{\sigma_y\left(\frac{b^2}{r^2}-1\right)\left[1-\frac{c^2}{b^2}+2\ln\frac{c}{a}+(1-\nu^2)\frac{E^p}{E}\left(\frac{c^2}{a^2}-\frac{c^2}{b^2}\right)\right]}{2\left(k^2-1\right)\left[1+(1-\nu^2)\frac{E^p}{E}\right]}-\frac{\sigma_y c^2\left(b^2-r^2\right)}{2b^2r^2}-\frac{P\left(\frac{b^2}{r^2}-1\right)}{k^2-1} \tag{25}$$

$$\sigma_{\theta f}=\frac{-\sigma_y\left(\frac{b^2}{r^2}+1\right)\left[1-\frac{c^2}{b^2}+2\ln\frac{c}{a}+(1-\nu^2)\frac{E^p}{E}\left(\frac{c^2}{a^2}-\frac{c^2}{b^2}\right)\right]}{2\left(k^2-1\right)\left[1+(1-\nu^2)\frac{E^p}{E}\right]}+\frac{\sigma_y c^2\left(b^2+r^2\right)}{2b^2r^2}+\frac{P\left(\frac{b^2}{r^2}+1\right)}{k^2-1} \tag{26}$$

According to Tresca yield criterion, the equivalent stress σ_{eq} can be defined as:

$$\sigma_{eq}=\sigma_\theta-\sigma_r \tag{27}$$

If the cylinder is intended to remain elastic throughout the loading process of the cylinder, then the equivalent stress should not exceed the yield stress of the material, i.e.:

$$\sigma_{eq}=\sigma_\theta-\sigma_r\le\sigma_y \tag{28}$$

3. Optimization problem definition

In the optimization problem, the variables vector is defined as:

$(X) = (x_1 \quad x_2 \quad x_3)^T$

In which $x_1 = a$ is the inner radius of the internal cylinder, $x_2 = c$ is the radius of elasto-plastic junction and $x_3 = b$ is the outer radius of the cylinder. The objective function, $f(x)$, is the weight of compound cylinder. The constraints of the problem are defined as follow:

1- $g_1(X) = \sigma_{eq}\big|_{r=x_1} - \sigma_y \le 0$. This implies that equivalent stress at the inner surface of the cylinder should not exceed the yield stress, σ_y.

2- $g_2(X) = \sigma_{eq}\big|_{r=x2} - \sigma_y \le 0$. This implies that equivalent stress at the outer surface of the cylinder should not exceed the yield stress, σ_y.

3- $g_3(X) = u_r\big|_{r=x1} - u_a \le 0$. This is an optional constraint implying that the radial displacement at the inner radius of compound cylinder must remain less than a specific value, u_a.

4- x_1 and x_3 have always to be positive and are forced to remain within the range $a_1 \le x \le a_2$.

5- x_2 must be less than the outer radius and greater than the inner one.

The optimization problem can be summarized as follows:

Minimize: $f(x) = \pi \cdot \gamma \cdot (x_3^2 - x_1^2)$ Subject to:

$$g_1(x_1,x_2,x_3) = \sigma_{eq}\big|_{r=x1} - \sigma_y \le 0$$
$$g_2(x_1,x_2,x_3) = \sigma_{eq}\big|_{r=x2} - \sigma_y \le 0$$
$$g_3(x_1,x_2,x_3) = u_r\big|_{r=x1} - u_a \le 0$$
$$g_4(x_1,x_2,x_3) = a_1 - x_1 \le 0$$
$$g_5(x_1,x_2,x_3) = x_1 - x_2 \le 0$$
$$g_6(x_1,x_2,x_3) = x_2 - x_3 \le 0$$
$$g_7(x_1,x_2,x_3) = x_3 - a_2 \le 0$$

Where, γ is the specific weight of the cylinder.

SQP technique [17 & 18] was employed for optimization process which was performed using MATLAB software.

4. Material and specimens

Two materials, aluminum and steel were used for optimization purposes. The material's properties are exactly the same as those used by Majzoobi and Ghomi [21].

The material's properties and the geometry of the specimens (only aluminum alloy) used for bursting tests were different from those used for optimization purposes. Figure 1 illustrates the shape of the specimens adopted from the work of Manning [19 & 20]. The ratio of inner to outer radii was 2.2, k=b/a=2.2, for all specimens. The material had a yield stress of $\sigma_y = 190\text{MPa}$. Figure 1 shows two specimens, one before testing and one after bursting. The gauge length of the specimens was 70 mm for all specimens.

Fig. 1: Two specimens before and after testing

5. Optimization results

The optimization problem defined in section 4 was performed for aluminum and steel cylinders with a=0.01 m, b=0.022 m under the following conditions:

Table 1:
The results for aluminum cylinders

P_i (MPa)	b(m)	c(m)	k	W (kg/m)	$r_{j(opt)}$ (m)
30	0.0138	0.0129	1.38	0.77	0.0133
34	0.0144	0.0133	1.44	0.91	0.0139
38	0.0150	0.0138	1.50	1.06	0.0144
42	0.0157	0.0142	1.57	1.24	0.0150
46	0.0163	0.0147	1.63	1.41	0.0156
50	0.0170	0.0152	1.70	1.60	0.0162
54	0.0177	0.0157	1.77	1.81	0.0168
58	0.0184	0.0162	1.84	2.02	0.0175
62	0.0191	0.0167	1.91	2.25	0.0182
66	0.0199	0.0173	1.99	2.51	0.0189
70	0.0206	0.0178	2.06	2.75	0.0196
74	0.0214	0.0184	2.14	3.04	0.0204
76.5	0.0219	0.0187	2.19	3.22	0.0209

(a) elastic-perfectly plastic material:

The autofrettage pressure varied between 30 to 75.5 MPa for aluminum cylinders and between 300 to 600 MPa for steel cylinders. From the optimizations, the optimum value of the radius of elasto-plastic junction, c, and weight of the cylinder were obtained. The results and their comparison with those predicted by analytical approach given by Zhu and Yang [14] are summarized in Tables 1 and 2 and illustrated graphically in figures 2 & 3 for aluminum and steel, respectively.

Table 2:
The results for steel cylinders

P_i (MPa)	b(m)	c(m)	k	W (kg/m)	$r_{j(opt)}$ (m)
300	0.0151	0.0138	1.51	3.16	0.0145
350	0.0162	0.0146	1.62	4.01	0.0154
400	0.0172	0.0154	1.72	4.83	0.0164
450	0.0184	0.0162	1.84	5.88	0.0174
500	0.0195	0.0170	1.95	6.91	0.0186
550	0.0208	0.0179	2.08	8.20	0.0197
600	0.0220	0.0188	2.20	9.47	0.0210

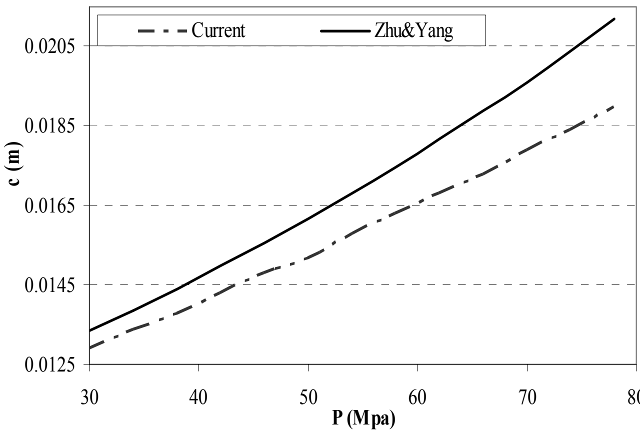

Fig. 2.Variation of c versus working pressure for aluminum cylinders

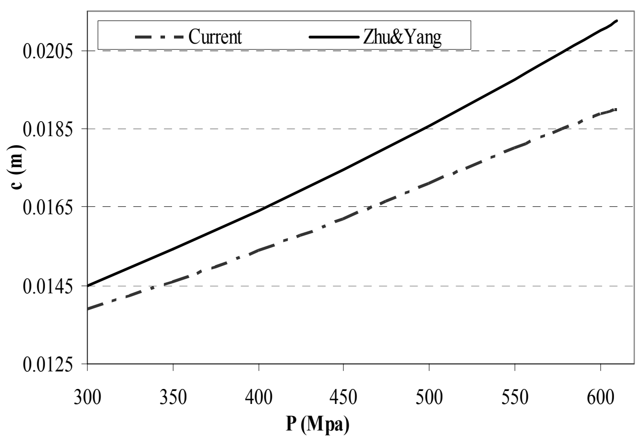

Fig. 3. Variation of c versus working pressure for steel cylinders

It can be seen from the tables and the figures that, in the first place, c increases as the working pressure increases, and in the second place, the average difference between the results obtained in this work and those given by Zhu and Yang is only 6.8% for aluminum and 7.4% for steel cylinders, respectively.

(b) elastic-plastic with linear strain hardening:

The results in this case are summarized in Tables 3 and 4 and depicted in figures 4 & 5 for aluminum and steel, respectively.

Table 3
The results for aluminum cylinders

P_i (MPa)	b(m)	c(m)	k	W (kg/m)	$r_{j(opt)}$ (m)
30	0.0138	0.0129	1.38	0.77	0.0133
34	0.0144	0.0134	1.44	0.91	0.0139
38	0.0150	0.0138	1.50	1.06	0.0144
42	0.0156	0.0143	1.56	1.22	0.0150
46	0.0163	0.0148	1.63	1.41	0.0156
50	0.0169	0.0152	1.69	1.57	0.0162
54	0.0176	0.0158	1.76	1.78	0.0168
58	0.0183	0.0163	1.83	1.99	0.0175
62	0.0190	0.0168	1.90	2.21	0.0182
66	0.0197	0.0173	1.97	2.44	0.0189
70	0.0204	0.0179	2.04	2.68	0.0196
74	0.0212	0.0184	2.12	2.96	0.0204
78	0.0219	0.0190	2.19	3.22	0.0212

Table 4
The results for steel cylinders

P_i (MPa)	b(m)	c(m)	k	W (kg/m)	$r_{j(opt)}$ (m)
300	0.0151	0.0139	1.51	3.16	0.0145
350	0.0161	0.0146	1.61	3.93	0.0154
400	0.0172	0.0154	1.72	4.83	0.0164
450	0.0183	0.0162	1.83	5.79	0.0174
500	0.0194	0.0171	1.94	6.82	0.0186
550	0.0206	0.0180	2.06	8.00	0.0197
600	0.0218	0.0189	2.18	9.25	0.0210
610	0.0220	0.0190	2.20	9.47	0.0213

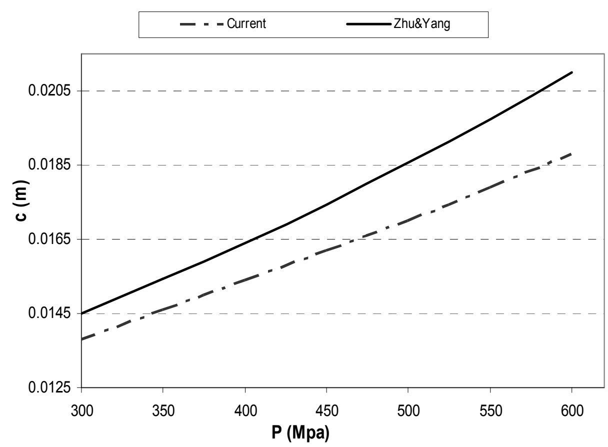

Fig. 4.Variation of c versus working pressure for aluminum cylinders

Again, the difference between the results obtained in this work and those given by Zhu and Yang is only 6.4% for aluminum and 7.1% for steel cylinders, respectively. Therefore, it may be concluded that (a) there is not significant difference between elastic perfectly plastic and elastic plastic with strain hardening material models for prediction of optimum radius of elastic plastic junction in autofrettage process and (b) the analytical results given by Zhu and Yang is confirmed by optimization results obtained in this investigation.

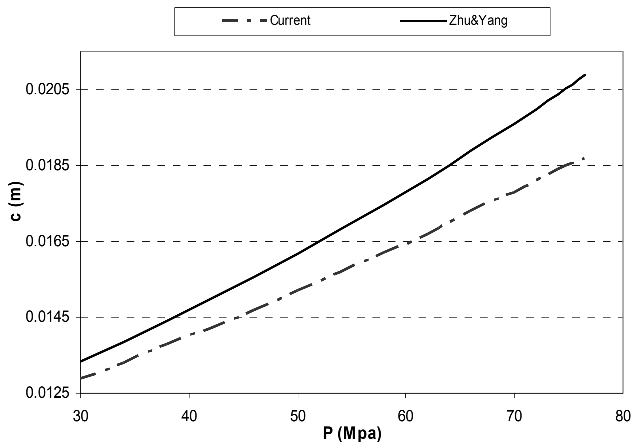

Fig. 5.Variation of c versus working pressure for steel cylinders

6. Numerical results

Single cylinders with the dimensions; a=0.1 m, b=0.2 m and an elastic perfectly plastic material's model with $\sigma_y = 800\ MPa$ were used for numerical modeling. The two pressure limits P_{y1} and P_{y2} can be computed as follows [1 & 21]:

$$P_{y1} = \frac{\sigma_y}{\sqrt{3}}(1-1/k^2) = \frac{800}{\sqrt{3}}\left(1-1/2^2\right) = 347 \text{ MPa}$$

$$P_{y2} = \sigma_y Ln(k) = 800\ln(2) = 555 \text{ MPa}$$

The cylinders were subjected to autofrettage pressures ranging from 350 MPa to 650 MPa. After removing the autofrettage pressure (AP), the cylinders were subjected to the working pressures of 100, 200 and 400 MPa. From the numerical simulations, the curve of von-Mises stress distribution was obtained for each autofrettage and working pressure (WP). From the curve, the value and the position of maximum von-Mises (MVS) stress were extracted. This stress and its position were then plotted versus autofrettage pressure for each working pressure. The results are shown in figure 6.

It is observed that for each working pressure, the MVS remains constant up to an autofrettage pressure which is nearly equal to P_{y1}. The curve then begins to decline to a certain point thereafter begins to rise or remain constant. It can be seen that for all WPs, the rising portion of the curves end at a point which is nearly equal to p_{y2}.

From the numerical results, it can be concluded that: (i) the MVS depends on the working pressure and for any WP, the best AP lies between P_{y1} and p_{y2}; (ii) for autofrettage pressures lower than P_{y1} and higher than p_{y2} the MVS remains unchanged); (iii) the position of MVS moves towards the outer radius as AP increases, and for autofrettage pressures higher than P_{y2} does not change

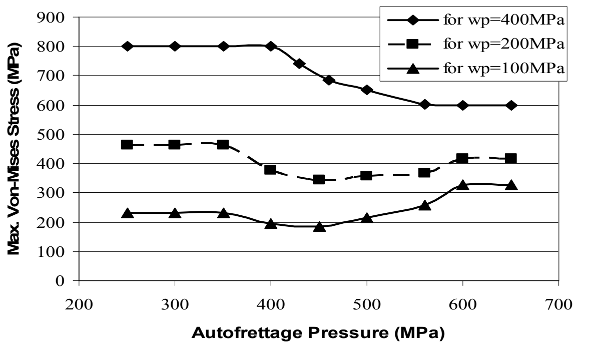

Fig. 6. Variation of maximum von-Mises stress versus autofrettage pressure at three working pressure

Now, Let examine the accuracy of equations for computation of optimum autofrettage pressure (Eq. 4) given by Zhu and Yang. For the material used in the numerical simulations, $\sigma_y = 800\ MPa$, and the working pressures, 100, 200 and 400 MPa, the optimum autofrettage pressures calculated from equation 4 and obtained from figure 6 are given in Table 5.

Table 5

Working pressure, p	100	200	400
p_{opt} (equation 4)	113	258	714
p_{opt} (figure 6)	440	450	550

The results given in Table 5 clearly show a distinct discrepancy between the optimum pressures predicteed by Zhu and Yang and the numerical results obtained in this work. As seen in the Table 5, the numerical results for optimum autofrettage pressures vary between $P_{y1} = 347$ MPa and $P_{y2} = 555$ MPa as calculated above. This is more consistent with experimental results given in the next section.

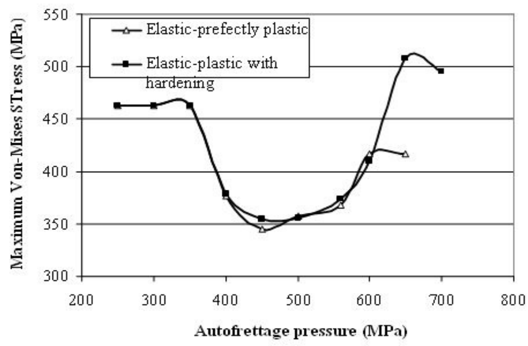

Fig. 7. Variation of maximum von-Mises stress versus autofrettage pressure two different material models

The results for elastic-pastic material with linear strain hardening are plotted in figure 7 for working pressure of 200 MPa. As the figure suggests, the two material models, yield nearly the same results for the minimum von-Mises stress and differ only at the autofrettage pressures higher than p_{y2} which are not of concern in this work. This trend was observeed for other working pressures.

7. Esperimental results

The experiments were carried out using a high pressure pump with a pressure capacity ranging from 1 to 275 MPa (40000 psi). The diag gauge of the pump had a minimum division of 3.5 MPa. Therefore an error of about ±1.75 MPa was expected for each reading. The bursting pressure for autofrettaged cylinders are given in Table 6. The results have been adopted from the work by Majzoobi *et al* [2]. In order to see the differences more clearly, the pressures are given in psi in parenthesis.

Table 6
(the values in parenthesis are in psi)

Autofrettage pressure	-	155.1 (22500)	124.1 (18000)	124.1 (18000)	137.9 (20000)	117.2 (17000)
Bursting pressure	148.2 (21500)	151.7 (22000)	155.1 (22500)	155.1 (22500)	162.0 (23500)	149.6 (21700)

The values of P_{y1} and p_{y2} as calculated from equations quoted above, are $P_{y1} = 115.2 MPa$ (16700 psi) and $p_{y2} = 150 MPa$ (21700 psi). It can be observed from Table 6 that the bursting pressure increases as autofrettage pressure rises but remains less than p_{y2}. However, when the pressure exceeds p_{y2}, the bursting pressure begins to decrease. This is quite consistent with the results extracted from figure 6. As it was explained in section 6, the minimum von-Mises stress lies between P_{y1} and p_{y2}. As working pressure increases, autofrettage pressure also increases and for high working pressures it approaches p_{y2}.

8. Conclusions

From the optimization, numerical and experimental results the following conclusion can be derived:
1- The optimum radius of elastic-plastic junction in autofrettaged cylinder does not differ significantly for elastic-perfectly plastic material compared with those obtained using an elastic-plastic with strain hardening material's model.
2- The results verify the analytical solution for optimizing the radius of elastic-plastic junction given by Zhu and Yang.
3- The optimum pressure predicted by Zhu and Yang are significantly different from the numerical predictions in this work.
4- The numerical results revealed that the optimum autofrettage pressure is obtained when von-Mises equivalent stress across the wall of the cylinder attains its minimum value.
5- The numerical predictions are verified by experimental results.

Acknowledgements

The authors wish to thank Dr Maleki, the Dean of Fcaculty of Engineering, Bu-Ali Sina University for his support. They also like to thank Mr. Heidari for his contribution in preparation of specimens and conducting the experiments.

References

[1] T.Z Blazinski, Applied elasto-plasticity of solids, Hong-Kong: Macmillan, 1983.
[2] GH Majzoobi, GH Farrahi, AH Mahmoudi, A finite element simulation and an experimental study of autofrettage for strain hardened thick-walled cylinders, J. Mater. Sci. Eng. A., vol. 359 pp. 326-31, 2003.
[3] PCT. Chen, Stress and deformation analysis of autofrettaged high pressure vessels, ASME special publication, vol. 110, PVP. New York: ASME United Engineering Center; pp. 61-7, 1986.
[4] G.J. Franklin, JLM. Morrison, Autofrettage of cylinders: prediction of pressure, external expansion curves and calculation of residual stresses Proceeding of institute of Mechanical Engineers, vol. 174, pp. 947-74, 1960.
[5] G.H. Majzoobi, G.H. Farrahi, M.K. Pipelzadeh and A. Akbari, Experimental and Finite Element Prediction of Bursting Pressure in Compound Cylinders, International Journal of Pressure Vessels and piping, vol 81, pp. 889-896, 2004.
[6] J.F. Harvey, Theory and design of pressure vessels, New York: Van Nostrand Reinhold Company Ltd., 1985.
[7] Brownell LE, Young EH. Process equipment design. New York: John Wiley & Sons, 1959.
[8] G. Yu, Chemical pressure vessel and equipment (in Chinese). Beijing: Chemical Industrial Press, 1980.
[9] E. David, An overview of advanced materials for hydrogen storage, Journal of Material Processing Technology, vol. 162-163, pp. 169-177, 2005.
[10] H.H. Lee, J.H. Yoon, J.S. Park, Y.M. Yi, A study of failure characteristic of spherical pressure vessels, Journal of Material Processing Technology, vol. 164-165, pp. 882-888, 2005
[11] AP Boresi, OM. Sidebottom, FB Seely, JO Smith, Advanced Mechanics of Materials, 3rd edition. New York: John Wiley & Sons, 1978.
[12] F. Kong, Determining the optimum radius of the elastic-plastic juncture for thick-walled autofrettage cylinder by graphic method, (in Chinese), Petrochemical Equipment,; 15:11, 1986.
[13] S. Timshenko, Strength of Materials, New York: Van Nostrand Reinhold Company Ltd, 1978.
[14] Ruilin Zhu, Jinlai Yang Autofrettage of thick cylinders, International Journal of Pressure Vessels and Piping, vol. 75 , pp. 443-446, 1998.
[15] A. Ghomi, Optimum Design of Thick-walled Pressure Cylinders (in Persian), MS.c final project, Bu-Ali Sina University, Hammadan, Iran, 2005.
[16] R. Ragab, S. E. Bayomi, Engineering Solid Mechanics: fundamentals and applications, Boca Raton CRC press, 1998.
[17] N. Garret and V. Anderplatts, Numerical optimization Techniques for Engineering design with applications, Mc-Graw-Hill, New York, 1989.

[18] Edgard Himmelblan, Optimization of Chemical Processes, McGraw-Hill, 1989.
[19] WRD Manning, S. Labrow, High pressure engineering. London: CRC Press; 1971.
[20] WRD Manning, Bursting pressure as the basis for cylinder design, Trans ASME, J Pressure Vessel Technology, vol. 100, pp. 374-81, 1978.
[21] GH. Majzoobi, A. Ghomi, Optimization of compound pressure cylinder, , Journal of Achievements in Materials and Manufacturing Engineering, In press, 2006.